

# Sequences of Passively Stable Dynamic Equilibria for Hybrid Control of Reconfigurable Spacecraft

Joseph P. Shoer\* and Mason A. Peck†  
 Cornell University, Ithaca, NY, 14853

This paper proposes a novel hybrid-control strategy to reconfigure modular spacecraft. This strategy utilizes passively stable system dynamics, which have the benefits of low control effort and a high degree of robustness. This approach treats reconfigurable spacecraft systems according to the theory of multibody kinematic mechanisms. It employs ambient force fields in the space environment (gravity gradient, magnetism, etc.), along with passively generated, non-contacting force fields on the spacecraft (such as those from permanent magnets), to drive the reconfiguration maneuver. The control strategy for reconfiguration in this paradigm consists of a selection of body incidences, joint Jacobians, and applied force fields that cause the multibody spacecraft system to evolve through passive dynamics to a new configuration. Many of these passive dynamical evolutions, chained together in stepwise fashion, allow the system to reach many possible desired configurations. All possible equilibrium configurations can be computed offline and uploaded to the spacecraft in a graph structure. The use of kinematic constraints and passive dynamics adds robustness to the system, while the stepwise nature of the reconfiguration maneuver provides many safe-hold points for verification regardless of transient dynamics.

## Nomenclature

$a, b$	= arc indices
$\mathbf{a}_1, \mathbf{a}_2$	= vectrices relating velocities and angular velocities to generalized coordinates
$\mathbf{b}_1, \mathbf{b}_2$	= vectrices relating accelerations and angular accelerations to generalized coordinates
$\mathbf{F}$	= force vector
$G$	= Newtonian gravitational constant
$\mathbf{H}$	= angular momentum vector
$i, j$	= body indices
$\mathbf{I}$	= inertia dyadic
$\mathbf{J}$	= single joint Jacobian matrix
$\mathcal{J}$	= collection of joint Jacobians for the entire spacecraft system
$M$	= planetary mass
$m$	= spacecraft mass matrix
$n$	= number of bodies in a multibody spacecraft system
$q$	= column matrix of generalized coordinates
$\mathbf{r}$	= position vector
$s$	= spacecraft body (vertex of multibody system graph)
$S$	= incidence matrix of a multibody system graph
$T_c$	= superconductor critical temperature
$u$	= kinematic joint or force element (arc on multibody spacecraft graph)
$U$	= potential energy
$\mu$	= transformation matrix between position relative to inertial space and position relative to the system center of mass
$\boldsymbol{\tau}$	= torque vector

\* Graduate Research Assistant, Department of Mechanical and Aerospace Engineering, 127 Upson Hall, Student Member AIAA.

† Assistant Professor, Department of Mechanical and Aerospace Engineering, 212 Upson Hall, Member AIAA.

$\omega$  = angular velocity vector

## I. Introduction

THE in-orbit reconfiguration of modular space systems is a very challenging problem in controls and dynamics. Solutions to this problem often involve a combination of multibody dynamics, multivariable controls, docking hardware and algorithms, state estimation, and the relative orbital dynamics of formation flight, expressed as a tracking problem.<sup>1,2,3,4,5,6</sup> These approaches incorporate interactions between many vehicles, sensors, and actuators, and thus may be both computation- and power-intensive with many potential points of failure. We wish to depart from this traditional methodology by focusing on the passive dynamics—and kinematics—governing multibody spacecraft systems. In this framework, a reconfiguration maneuver is a sequence of natural, dissipative motions towards passive equilibria of the multibody system. The particular desired sequence and location of these equilibria are explicitly defined by augmenting the passive system dynamics with non-contacting force fields, some of which occur in nature. In this manner, spacecraft composed of many modules can execute complex but failure-robust reconfiguration maneuvers with little to no control computation or actuation. Any required computations can be performed offline with common multibody dynamics techniques. Operators on the ground can verify the system state while it is paused at any “safe step” intermediate equilibrium. This reconfiguration technique thus adds robustness, determinacy, and power savings to the reconfiguration process.

There is a parallel between this reconfiguration concept and mechanical deployments in which the potential energy provided by a spring causes a joint to move to a passive dynamic equilibrium. In general, such an approach to reconfiguration may apply to any modular spacecraft system in which kinematic joints link the modules; however, it is especially relevant to systems with modules connected by non-contacting force fields through one of several enabling technologies. Such systems include Coulomb-tether formations<sup>7</sup> and Electromagnetic Formation Flight,<sup>8</sup> both of which involve active control strategies, reducing the benefits of reconfiguration through passive dynamics. Alternatively, a modular space system linked with magnetic flux pinning is both passively stable and non-contacting, with inter-module separation ranges up to tens of centimeters.<sup>9,10,11</sup> These systems blur the distinction between modular systems of docked spacecraft and formation-flying spacecraft,<sup>12</sup> with varied applications ranging from particulate solar sails<sup>13</sup> to sparse-aperture telescopes.<sup>14</sup>

Magnetic flux pinning is an interaction between type II high-temperature superconductors (HTSCs) and magnetic fields. All superconductors repel weak magnetic fields because the fields excite supercurrent loops within the zero-resistance HTSC. The magnetic field generated by these supercurrents exactly opposes the applied field, causing the net field within the HTSC to be zero; this repulsion is known as the Meissner effect.<sup>15,16</sup> Type II HTSCs such as yttrium barium copper oxide (YBCO), however, are laced with impurities that form sites where sufficiently strong magnetic fields, with flux density above an HTSC-specific critical value,<sup>18</sup> penetrate the superconducting material. The applied magnetic field lines become trapped on these impurities in the HTSC; supercurrents excited by the applied field oppose any motion of the flux lines away from such “pinning” sites.<sup>15</sup>

The most readily observed macroscopic behavior of flux pinning is the levitation of a permanent magnet over an HTSC. After the field lines of the magnet are pinned, the superconductor resists any change in the magnetic flux distribution within its volume. This resistance comes from shifts in the distribution of supercurrents within the HTSC, and it manifests itself as a force and torque on the magnet. The magnet experiences a nonlinear, hysteretic restoring force pushing it towards a six-dimensional equilibrium and a strong damping force similar to eddy-current damping. A simple (and effective, for small motions) model of a flux-pinned magnet-superconductor pair connects the two bodies by a multiple-degree-of-freedom (DOF) spring and damper.<sup>17,18</sup> The linear stiffness of a flux-pinned magnet-superconductor pair depends on the size and separation of the two objects and can exceed hundreds of newtons per meter.<sup>9,10</sup>

Flux pinning is ideal for space assembly applications. It can create passively stable 6DOF equilibria among multiple bodies in space since the magnetic field of the supercurrents depends on the three-dimensional positions, orientations, and motions of flux-pinned magnets. In addition, this effect does not require power. As long as the HTSC remains in its superconducting state (that is, below its critical temperature:  $T_c \approx 88$  K for YBCO), it pins magnetic flux. No voltage need be applied to the superconductor, and no actuation of the magnet is required to maintain the flux pinning. The temperature dependence of flux pinning means that HTSCs may require power for cooling if they receive incident sunlight; so, a sunshade may be sufficient to maintain superconductor temperatures below  $T_c$ . Cooling and warming the superconductors is thus a means to toggle inter-module interfaces.

The power and fuel savings for formation flight missions would be significant, and substantial mass savings may be realized by using flux-pinned interfaces instead of conventional docking hardware or conventional attitude control systems on modular or formation-flying missions. Flux-pinned interfaces also add the prospect of passive

stability following any of several power- or propulsion-related failures, an attractive possibility for any spacecraft that requires fault tolerance. Data and software-related failures would not result in instability in such a system.

The stiffness and damping properties of the flux-pinning interaction depend on the shape of the magnetic field pinned to the superconductor: in particular, flux-pinning stiffness in any DOF is a function of the magnetic field gradient along that DOF. Shaping a magnetic field pinned to a HTSC therefore introduces or removes stiffness, creating a reconfigurable, non-contacting, kinematic mechanism.<sup>11</sup> Additional shaping of the magnetic fields, along with exploitation of rigid-body dynamics, gravity gradient, and other ambient forces, may change the stability of the equilibrium points of these mechanisms. Control of a reconfiguration maneuver for such a system therefore takes the form of specified magnetic-field geometries at each interface. The specifics are chosen to introduce or stiffen appropriate kinematic degrees of freedom, with accompanying magnetostatic, electrostatic, gravitational, or Coriolis forces that cause the system to passively “fall” towards a desired equilibrium in configuration space. Multiple steps between sequential equilibria allow the system to reach many possible configurations. In these non-contacting systems, spacecraft assembly can be executed as a similar sequence, with modules falling into 6DOF basins of attraction.

This paper is concerned with the development and implementation of this passive reconfiguration technique. Section II discusses the mathematical theory for applying force fields to create appropriate potential minima in configuration space. That section also discusses approaches for chaining together a sequence of passively stable equilibria to reach a wide range of possible final configurations. Finally, Section III describes simulations and experiments that demonstrate many of the concepts described in this paper.

## II. Potential-Augmented Configuration Space

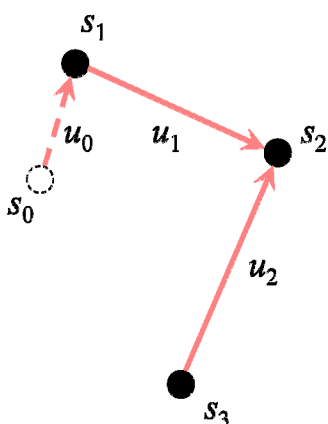


**Figure 1. Graph description of a multibody system.**

A single point in an  $n$ -dimensional configuration space may represent the physical configuration of a multibody system. The configuration space may take the form of ordered  $n$ -tuples of, for example, joint angles and offsets.<sup>19</sup> Configuration space is thus related, but not identical, to state space. In Hamiltonian dynamics, the configuration space often appears embedded in higher-dimensional Euclidian space and is weighted by the kinetic energy of the system; this weighted surface is called the configuration manifold and represents all the possible trajectories of a physical system.<sup>20</sup>

The architecture of a reconfigurable space system in this paradigm is based on kinematic constraints that define the locus of possible points in configuration space. In Hamiltonian language, the kinematic constraints determine the shape of the configuration manifold embedded in higher-dimensional space. In this treatment, kinematic constraints appear as boundaries of the configuration space. The system may move continuously from point to point in configuration space as both external and internal forces act on the system, in accordance with the laws of motion. An important point for this reconfiguration concept is that specified alterations of the kinematic constraints are part of the control effort on the multibody system. That is, some of the control laws acting on the system involve changing the allowed trajectories in configuration space so that the system approaches a desired configuration.

Concepts from graph theory capture multibody systems in a mathematical framework, as shown in Figure 1. With each of the  $n$  bodies denoted by  $s_i$  and each joint (or “arc”) linking two bodies by  $u_a$ , an incidence matrix  $S$  expresses the connections between joints and bodies. An element  $S_{ia}$  takes the values of 0 if arc  $a$  is not incident with body  $i$ , +1 if arc  $a$  goes out from body  $i$ , and -1 if arc  $a$  goes in to body  $i$ . The body  $s_0$  is a fictitious base body linked to the system by a fictitious joint  $u_0$ . The equations of motion for the entire system include the information in the incidence matrix: Wittenburg<sup>21</sup> gives the equations of motion for a multibody system without constraints to inertial space as

$$\left\{ \mathbf{a}_1^T \boldsymbol{\mu} \cdot m \boldsymbol{\mu}^T \mathbf{a}_1 + \mathbf{a}_2^T \cdot \mathbf{I} \cdot \mathbf{a}_2 \right\} \ddot{\mathbf{q}} = \mathbf{a}_1^T \boldsymbol{\mu} \cdot \left( \mathbf{F} - m \boldsymbol{\mu}^T \mathbf{b}_1 \right) + \mathbf{a}_2^T \cdot \left( \boldsymbol{\tau}^* - \mathbf{I} \cdot \mathbf{b}_2 \right), \quad (1)$$

in terms of the applied force  $\mathbf{F}$  and torque  $\boldsymbol{\tau}$  vectrices, the system mass properties  $m$  and  $\mathbf{I}$ , the transformation to motion relative to the center of mass  $\boldsymbol{\mu}$ , the generalized coordinates  $q$ , and the matrices governing the relations

$$\begin{aligned}\dot{\mathbf{r}} &= \mathbf{a}_1 \dot{q} & \ddot{\mathbf{r}} &= \mathbf{a}_1 \ddot{q} + \mathbf{b}_1 \\ \boldsymbol{\omega} &= \mathbf{a}_2 \dot{q} & \ddot{\boldsymbol{\omega}} &= \mathbf{a}_2 \ddot{q} + \mathbf{b}_1.\end{aligned}\quad (2)$$

In Wittenburg's notation,  $\boldsymbol{\tau}^*$  is the vectrix composed of the elements  $\boldsymbol{\tau}_i - \boldsymbol{\omega}_i \times \mathbf{I}_i \cdot \boldsymbol{\omega}_i$  for each body. The transformations in Eq. (2) include the incidence matrix as well as the individual Jacobian relationships of each joint in the multibody system. The matrix equation of motion (1) has as many rows as there are degrees of freedom in the entire system, so the generalized joint coordinate matrix  $q$  is an expression of a point in the configuration space for the system.

Given a multibody system represented by a point in configuration space, let us now introduce force fields to augment its dynamics with a potential function. This potential function is a scalar value associated with each point in configuration space, resulting from an application of internal or external forces or torques to the system—for instance, the effective potential energy of the system in circular orbit around a planet:<sup>22</sup>

$$\begin{aligned}U_{eff} &= \sum_{i=1}^n \left( \frac{H^2}{2 \left( \frac{Mm_i}{M+m_i} \right) |\mathbf{r}_i|^2} + \frac{GMm_i}{|\mathbf{r}_i|} \right) \\ &= f(q).\end{aligned}\quad (3)$$

Now, depending on the shape of the potential function, there may be dynamic equilibria in configuration space, represented by minima or “wells” in the potential. A system with such equilibria naturally moves towards these equilibria and, assuming that the system is dissipative, settles into the potential well in steady state. The following three steps identify the possible reconfiguration maneuvers a system may undergo:

1. Determine, from the possible kinematic constraints on the system, the allowed trajectories of the system in configuration space.
2. Set up a potential to create a stable equilibrium at a location in configuration space. Allow the system to settle into the resulting potential well.
3. If necessary, identify any newly allowed trajectories in configuration space and repeat some combination of the first two steps to move the system to another point in configuration space.

The applied control input at each discrete step in this process consists of a collection  $\{\mathcal{S}, \mathbb{J}, U(q)\}$ : the incidence matrix  $\mathcal{S}$ , the set of all joint Jacobians  $\mathbb{J} = \{J_0, \dots, J_n\}$  and the potential  $U(q)$  from the applied force fields. At each stepping-stone configuration, the input incidence, Jacobian set, and potential must be chosen from all allowable selections for that point in configuration space. Changes to the incidence matrix in general depend on the proximity of the various bodies. Changes to the Jacobian set depend on the properties of the joints in question. Changes to the potential function depend on the environment around the spacecraft and what force fields the spacecraft can generate. In this mathematical treatment, any potential energy function  $U(q)$  is acceptable, but the following analysis assumes that  $U(q)$  is selected from a finite set of possible functions related to the spacecraft capabilities and environment.

As long as the individual steps in the reconfiguration process consist of stable dynamics, the entire reconfiguration maneuver is stable. If the system switches to a new set of dynamics only after transient motions damp out, then any stepping-stone sequence of passively stable dynamics is itself passively stable.<sup>23</sup> More generally, a stepwise reconfiguration maneuver in which one potential  $U$  is present at all points in the maneuver is stable in the global Lyapunov sense of hybrid systems, with the system's total energy as the global Lyapunov function

$$V(x, \dot{x}) = \frac{1}{2} \dot{x}^T M \dot{x} + U(x), \quad (4)$$

where  $x$  is the system state vector and  $M$  is a system mass matrix. This function always decreases in a dissipative system, as the system approaches stable equilibrium. In fact, the stepwise reconfiguration is always stable, even if energy is added by selection of a new potential  $U$  that is discontinuous with the previous potential. The reason is that the system energy is always decreasing and ends up at a lower value overall as the system comes to the stable equilibrium at the end of the stepwise reconfiguration maneuver. Thus the system is stable in the multiple Lyapunov function sense, with the multiple Lyapunov functions formulated as in Eq. 4 with substitution of the proper  $U(x)$ .<sup>23</sup>

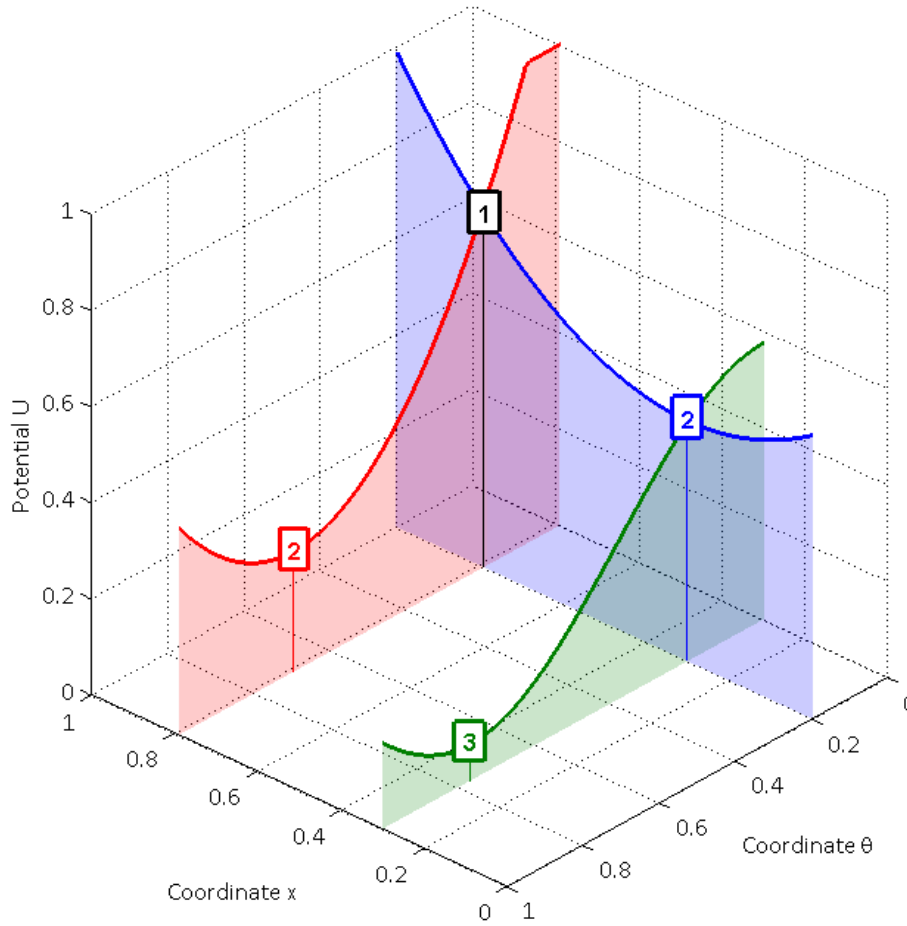


**Figure 2. Illustration of the stepwise passive reconfiguration concept in a system with two possible degrees of freedom augmented with potentials.**

The principles of hybrid automata<sup>24</sup> apply to this description in a straightforward manner. The continuous modes of the automaton are the sets of dynamics with a given incidence matrix and Jacobian set. That is, the modes are the dynamics of the system at any configuration-space equilibrium, as well as the dissipative transition to that equilibrium. The possible collections  $\{S, J\}$  are the guards enabling discrete transitions. The invariants that cause the automaton to perform a discrete transition are conditions that the current configuration must be at a potential minimum  $q_{eq} = (q|U(q) = \min U)$ . The control strategy in this paper involves manipulating the invariants and guards to guide the hybrid execution of the automaton to a continuous mode with a desired equilibrium configuration  $q$ .

Let us consider as an illustration of the process a system consisting of two bodies in free space, with one of two possible joints linking them together. These possible joints are distinguished by the coordinates  $x$  and  $\theta$  for uniqueness. These designations also illustrate a possible architecture of the system: the bodies may be connected by either a prismatic joint (coordinate  $x$ ) or a revolute joint (coordinate  $\theta$ ). The configuration space of the system then consists of the  $(x, \theta)$  plane. Control of this system involves the choice of joint ( $x$  or  $\theta$ ) and the application of an arbitrary force field to establish a potential function along the line of allowed configurations. If the system starts at Point 1 in configuration space (Fig. 2), then there are two possible trajectories of the system configuration: either a line in  $x$  or a line in  $\theta$ , depending on the enabled guard in the hybrid automaton. The choice of potential function, either the red or blue curve in the figure, causes a discrete transition and move the system from Point 1 to either Point 2 on the red curve in  $\theta$  or Point 2 on the blue curve in  $x$ . This process may involve transient dynamics; the reconfiguration sequence does not proceed to the next maneuver until the system has reached steady state. If the new configuration is not the desired final configuration of the system, another selection of kinematic constraints and

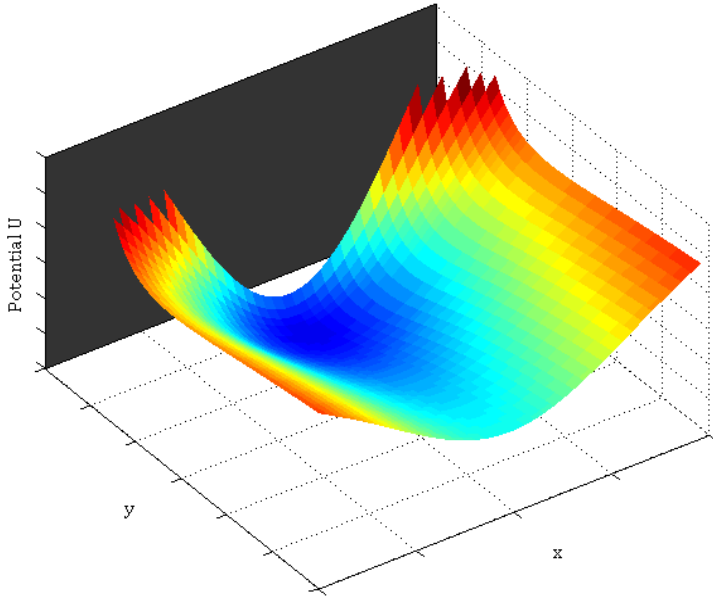


**Figure 3. Illustration of the magnetic potential well linking a flux-pinned magnet and superconductor. The superconducting plane is shaded.**

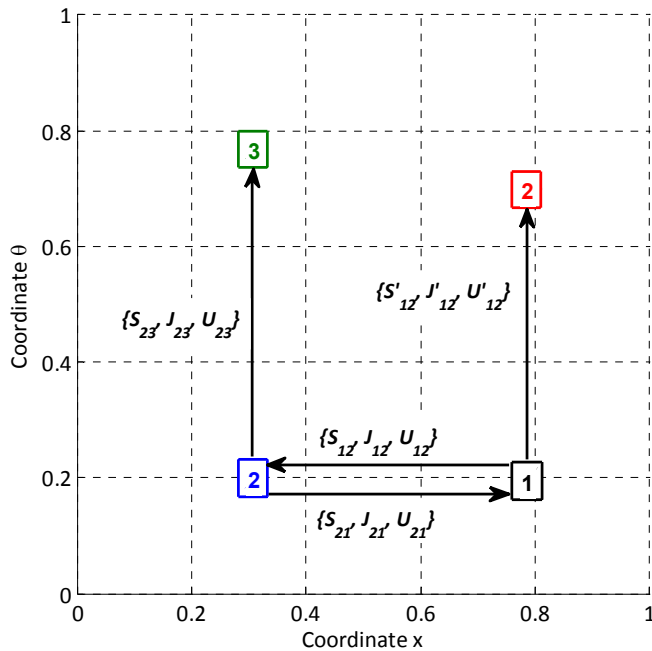


**Figure 4. Example reconfiguration graph for the system from Fig. 2, superimposed on configuration space.**

positioned with respect to the superconductor in the remaining four degrees of freedom as well. Establishing such stable potential wells is critical to enabling reconfiguration with no active control, as it is the passive stability of these wells that allows this control strategy to ignore the continuous-time dynamics of the system when it moves from point to point in configuration space.

potential function may cause the system to move to yet another configuration, such as from Point 2 on the blue curve to Point 3 on the green curve.

This example shows that system cannot reach Point 3 directly from Point 1 (assuming, of course, that either a revolute or prismatic joint, but not both, is allowed). In a more complex system, kinematic constraints may not just change in character but may also appear and disappear. Thus, some configurations are impossible to reach directly from an initial configuration, and intermediate steps are necessary. This situation occurs in the case of a system that engages and disengages some of its joints (altering its incidence matrix) as the component bodies come close to or separate from one another.

The example also makes clear that this control strategy does not require any sensing, computation, or feedback actuation of the system when the states are between equilibria. This concept requires only knowledge of the initial and final configurations for each step in the process. It is a hybrid control scheme in which the continuous-time dynamics of the system are less relevant than the configuration space points at which the system dynamics change. On a space system with limited computation capabilities, the locus of possible reconfiguration sequences may be determined on the ground and either be transmitted on an as-needed basis or be stored in spacecraft memory as a compact lookup table.

Flux pinning is particularly attractive for this approach to reconfiguration because it provides a means to establish stable potential wells in all six rigid-body degrees of freedom. Figure 3 shows a sketch of the potential well binding a flux-pinned permanent magnet to a superconducting plane in translation space,  $U(x, y)$ . A frozen-image model of flux pinning generated the data for this plot.<sup>9,25</sup> If the magnet does not have an axisymmetric field, similar potential wells keep the magnet stably

This control architecture is based on a large collection of equilibria in configuration space, and the identification of reachable equilibria from the current system configuration. Graph theory provides a convenient language to describe the equilibria and the control inputs necessary to move the spacecraft system from one to another. In this paradigm, each reconfigurable space system has an associated “reconfiguration graph.” The vertices of the reconfiguration graph represent each of the possible passively stable potential wells of the system in configuration space  $q$ , while the directed arcs represent the collections  $\{S, \mathbb{J}, U\}$  that take the system from one configuration  $q$  to another  $q'$  (see Figure ). For application in a spacecraft system, the graph is constructed offline according to the three-step process described above. Important questions for reconfiguration control, such as which configurations are reachable from a given initial configuration and which configurations, if any, are “sinks” from which the system cannot proceed further, are answered by this graph. The graph-based approach highlights how this reconfiguration paradigm allows spacecraft or spacecraft operators to concentrate on reconfiguration tasks from a high level, relegating the low-level evolution of the system from one configuration to another to kinematics and passive dynamics.

Figure 5 shows a temporal simulation of the configuration-space behavior of the system diagrammed in Fig. 2 and Fig. 4. The system begins at configuration point 1. At time  $t = 100$  s, the system receives the discrete control input  $\{S_{12}, \mathbb{J}_{12}, U_{12}\}$ , which takes it to configuration 2 on the reconfiguration graph. The incidence matrix and Jacobian allow motion only along coordinate  $x$  in configuration space, and the potential establishes point 2 as a stable equilibrium (Fig. 2). With dissipation, the dynamics of the system cause it to settle into the new equilibrium configuration after some settling time. At this intermediate point, the spacecraft control processor or ground operators have the option of safely pausing the sequence and verifying the system configuration since the system is in a stable equilibrium. In this simulation, the system receives a new input  $\{S_{23}, \mathbb{J}_{23}, U_{23}\}$  at  $t = 600$  s. The system Jacobian now allows motion in coordinate  $\theta$  only, and the new potential energy function changes the position of the stable equilibrium in configuration space. Once the transient response decays, a final control input  $\{S_f, \mathbb{J}_f, U_f\}$ , likely consisting only of the Jacobian set  $\mathbb{J}_f$  to lock out further motions and maintain the final configuration. The system relies on the selection of joint kinematics and the properties of the potential well to ensure that there are no collisions or other adverse effects during the transient time evolution, which proceeds without the need for any continuous control inputs or sensing.

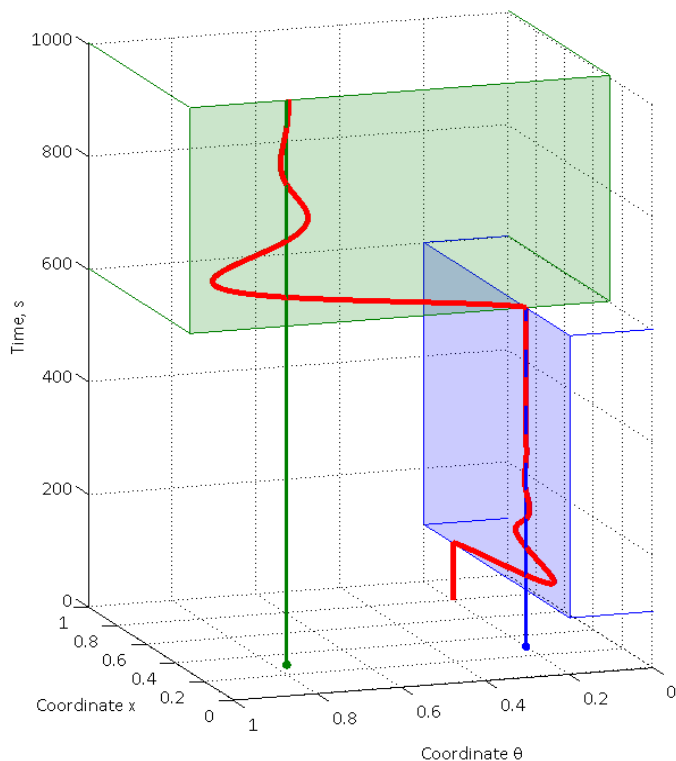


**Figure 5. Sample time history of a reconfiguration of the system from Fig. 2. At  $t = 100$  s, the control input is  $\{S_{12}, \mathbb{J}_{12}, U_{12}\}$  and at  $t = 600$  s, it is  $\{S_{23}, \mathbb{J}_{23}, U_{23}\}$ .**

### III. Simulation and Testbed

A simulation of a simple case demonstrates the advantages of this spacecraft reconfiguration approach in terms of stability and control effort. The simulated situation is that of three cube-shaped spacecraft modules that begin in a line, reconfigure into an “L” shape, and then return to their original configuration. The spacecraft modules are 1 kg each and orbit the Earth at a typical LEO altitude in the presence of gravity gradient. The spacecraft also have physical features on each cube face to lock edges together with stiffness and damping (via flux pinning, for example) or to rotate freely about a cube edge. While the spacecraft in the rotating mode, the simulation allows the spacecraft to either repel or attract nearby faces of other spacecraft cubes with a constant magnetic field, such as that of two permanent magnets or two electromagnets with a constant current.

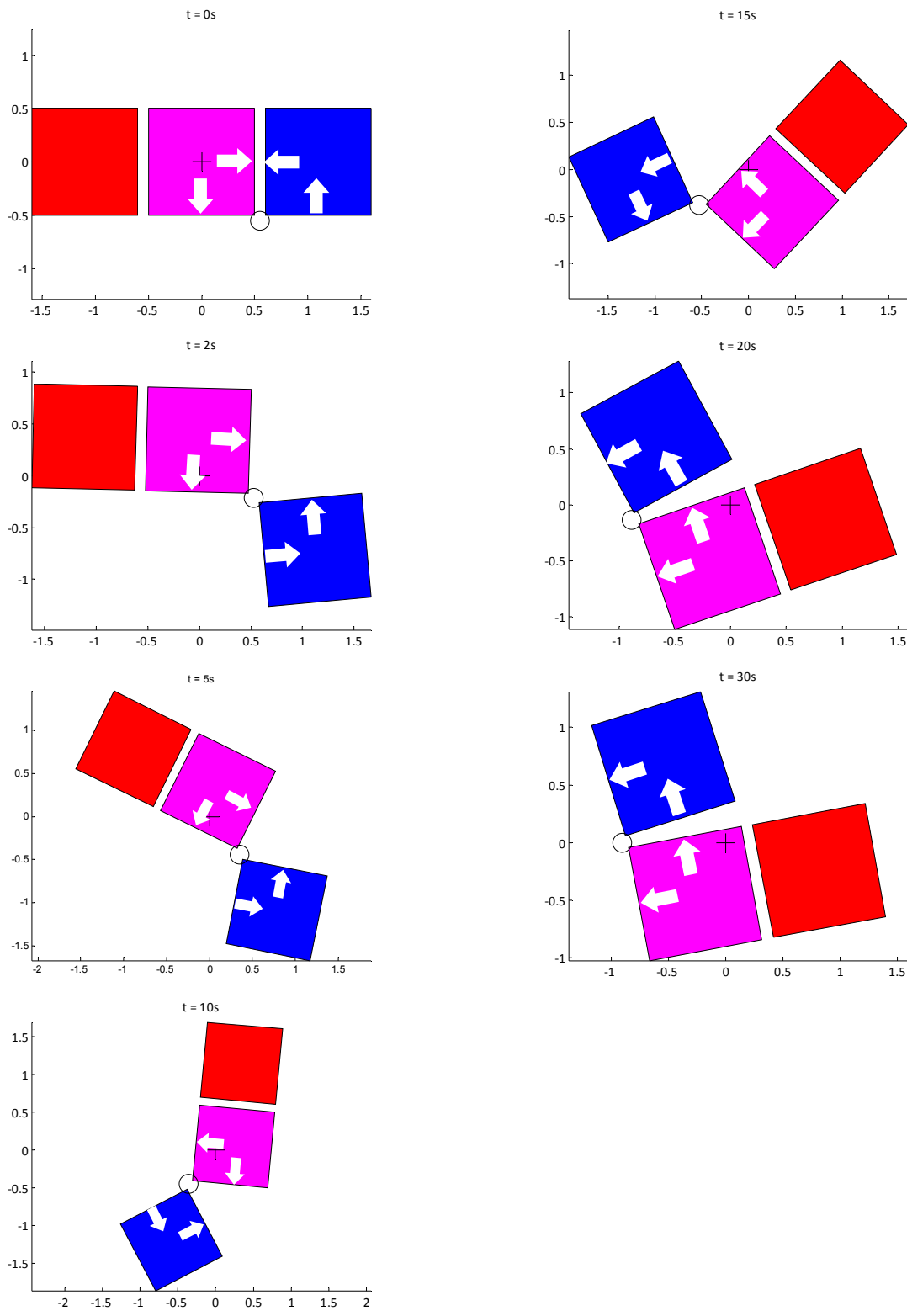


**Figure 6. Time-lapse images of the simulated reconfiguration maneuver. The circle represents the revolute joint, and the cross marks the system center of mass; the Earth is in the negative  $x$  direction. Arrows indicate the polarity of magnetic fields.**

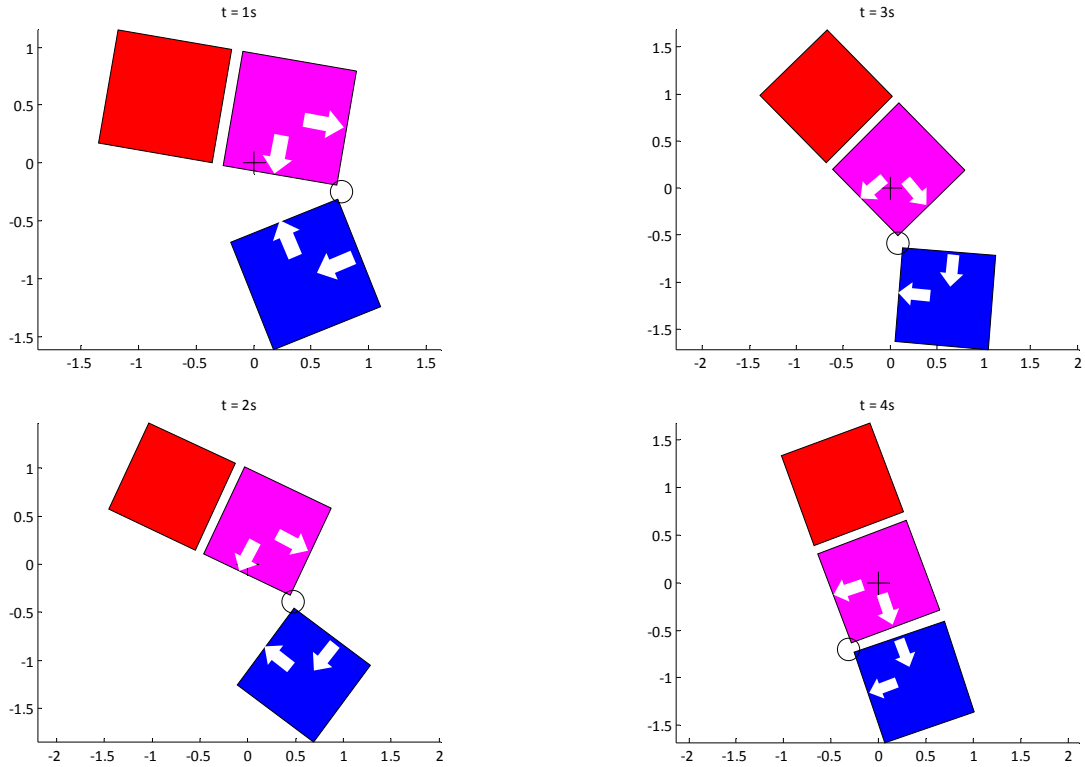


**Figure 7. Temporal snapshots of the simulated reconfiguration maneuver. The circle represents the revolute joint and the cross marks the system center of mass; the Earth is in the negative  $x$  direction. Arrows represent the polarity of magnetic fields.**

The system begins in a gravity-gradient stabilized orbit for the first half of the simulation (Figure ), in which the system moves from a linear configuration to an “L” configuration. The two spacecraft modules closest to the Earth always remain with their faces locked together, while the outermost spacecraft is connected to the middle spacecraft with a revolute joint after time zero. From time  $t = 0$  s to 20 s, a constant magnetic field repels the outermost cube from the initially adjacent face on the middle cube and attracts it to face 90 degrees clockwise from the initial location. The combined forces of magnetism and gravity gradient draw the hinged halves of the modular spacecraft into the new “L”-shaped configuration. By  $t = 20$  s, the two hinged cubes are close enough to re-engage any flux-pinning or mechanical docking apparatus to lock the configuration in place. In the first ten seconds of this maneuver, both gravity gradient and magnetism work to assist the reconfiguration, while in the last twenty seconds, magnetism must overcome gravity gradient. The control sequence for this maneuver is realized through of a selection of joint Jacobian (changing a fixed joint between the middle and outer cubes to a revolute joint) and potential (gravity gradient plus magnetic potentials) at  $t = 0$  s, followed by a new selection of Jacobian (fixing the joint between the middle and outer cubes) at the end of the maneuver.

For the second half of the maneuver (Figure ), the revolute joint again connects the same two spacecraft cubes, but the magnets now have reversed polarity. The spacecraft system starts at the final configuration of the previous maneuver, and the cubes swing out into linear formation under the influence of the magnetic fields and gravity. This reconfiguration occurs much faster than the first, because the gravity gradient and magnetic forces always tend to pull the cubes away from the “L” and towards the line formation. The control sequence for this maneuver, like that of the previous one, results entirely from a selection of joint Jacobian and potential to enable and drive reconfiguration, followed by a final selection of Jacobian to end the maneuver at  $t = 4$  s. Note that the final formation in Figure is not yet gravity-gradient stabilized, but from the point onward, the spacecraft configuration remains fixed. Time histories of both maneuvers appear in Figure . These simulations illustrate how ambient force fields and open-loop control may be sufficient to manage reconfigurable space systems.

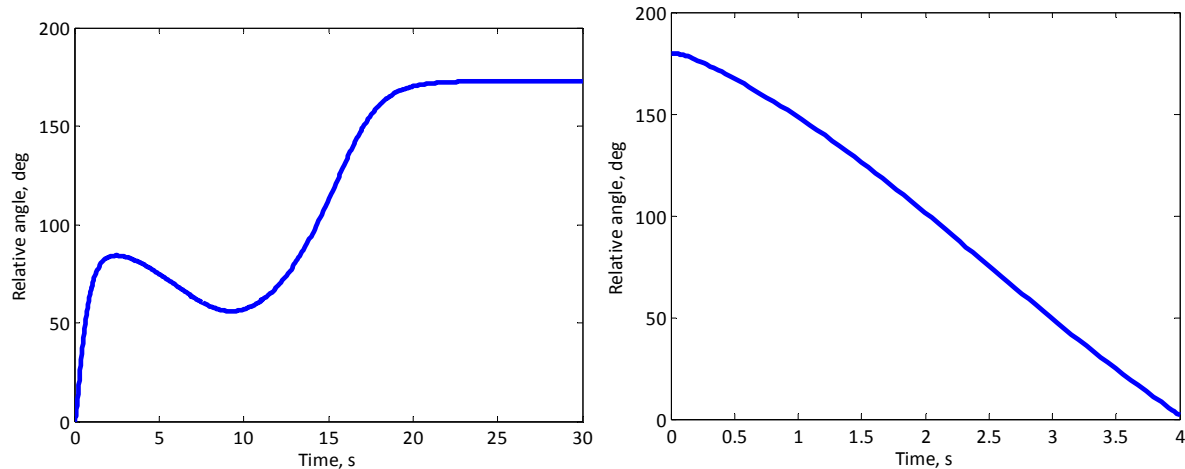


**Figure 8. Time histories of the reconfigurations in Fig. 6 and Fig. 7.**

A low-friction, air-levitated, three-degree-of-freedom (3DOF) testbed currently under development will provide experimental verification of this reconfiguration approach as well as data on power usage and control requirements. This testbed is similar to proof-of-concept demonstrations that use flux pinning to create simple kinematic mechanisms, but it is much more versatile, extensible, and includes more vehicles.<sup>11,26</sup> Each vehicle fits within a CubeSat-sized footprint (10 cm × 10 cm) and contains several modular attachment points that can be fitted with magnets, electromagnets, superconductors, reaction wheels, or other actuators. A computer controls the collection of vehicles wirelessly, and a motion-tracking camera system records the resulting motions.

Once complete, this testbed will incorporate any of several combinations of magnets, electromagnets, and flux-pinning superconductors that enable it to form various potential wells in translational and rotational degrees of freedom. Figure 9 shows several of the reconfiguration maneuvers that the system will perform using the theory developed in this paper. These maneuvers include:

- a) Passive self-assembly from a collection of free-flying vehicles into a modular structure “preprogrammed” by the specific arrangements of superconductors and magnets.
- b) “Walking” reconfigurations, in which one or more vehicles alternates the corner with revolute joint kinematic constraints in such a way that it walks around or along another vehicle or line of vehicles.
- c) Reconfigurations in which the vehicles form a common kinematic mechanism, such as a four-bar linkage.
- d) Reconfigurations in which the potential energy between vehicles causes them to fall into relative basins of attraction that result in a lattice-like structure, or reconfigurations in which the potential energy causes the vehicles to move from one lattice-like arrangement to another.

Finally, a 6DOF demonstration of these reconfiguration concepts will be conducted on the NASA microgravity simulator aircraft on 11-

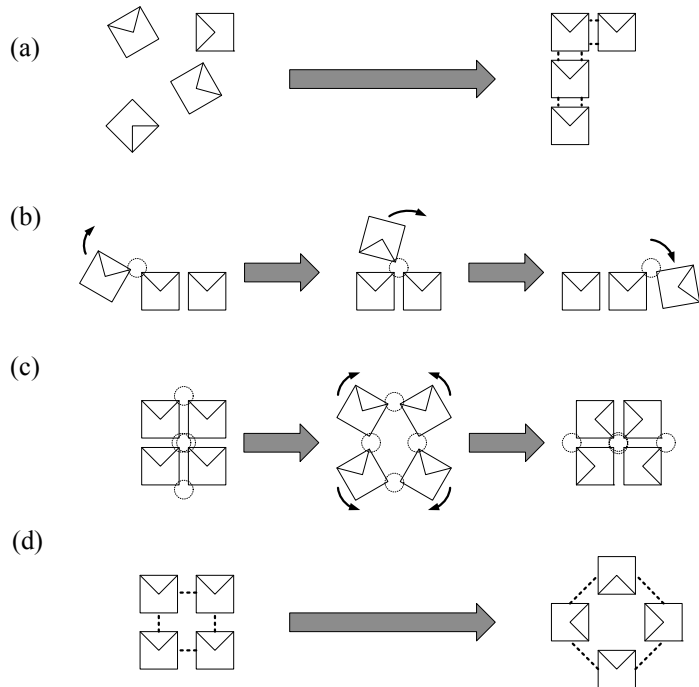


**Figure 9. Illustrations of testbed reconfigurations with 3-4 vehicles. Dotted lines represent stable 3DOF potential wells linking vehicles and dotted circles represent revolute joints.**

12 August 2009. This demonstration is expected to show the applicability of magnetic flux pinning to spacecraft docking and reconfiguration in freefall.

#### IV. Conclusion

The reconfiguration of multibody spacecraft systems in orbit will be an important part of future space development. Reconfiguration is related to the in-orbit docking, assembly, repair, and refurbishment of high-value systems and provides an avenue for small, responsive space systems to provide a wide range of functionality to meet many different missions. Low-power, robust approaches to space system reconfiguration will allow many future space systems to take advantage of these capabilities. These systems may include large-aperture, Earth-orbiting telescopes composed of small modules deployed in a phased manner to outer Solar System exploration missions. The discrete modules would enable the telescope to adapt to new mission roles and changing science targets. Human spaceflight activities will also benefit from failure-robust reconfiguration techniques that enable expansions to space stations or self-repair and adaptation of manned vehicles beyond low-Earth orbit.

The proposed method of reconfiguration from one shape to another is a stepwise sequence of kinematics and passively stable dynamics rather than an active tracking problem. A spacecraft system undergoing such a reconfiguration maneuver achieves low control and computation requirements by (1) taking advantage of the ambient force fields naturally present in the space environment, such as gravity, or (2) augmenting these forces with additional force fields from passive sources, such as permanent magnets. The passive dynamics of the system add robustness by reducing the number of actuators required for reconfiguration and placing the onus of regulating the maneuver on multibody kinematics rather than an on-board control system. This strategy gives the system determinacy in each step of the reconfiguration, in the sense that the system moves towards known dynamic equilibria. Operators can confirm the system configuration at each of these “safe steps.” Should any problem arise during the process, the spacecraft naturally falls into a stable equilibrium configuration, from which recovery operations can safely take place.

As this research continues, we will continue to develop mathematical and conceptual tools to express reconfiguration maneuvers as a stepping-stone sequence of passive evolutions to stable dynamic equilibria controlled by discrete selection of incidences, Jacobian sets, and potential energy between steps. These mathematical tools will include conditions on the stability, controllability, and reachability of stepwise passively reconfigurable systems, expressed in terms of the properties of the directed reconfiguration graph. For practical applications, we will develop algorithms to compute the reconfiguration graph vertices in configuration space and control inputs associated with each arc. These theoretical tools will have applications to more general reconfigurable systems than those linked by magnetic flux pinning or other non-contacting forces. They apply to any systems in which kinematic constraints can be altered, body incidences can be modified, or force fields can be applied. In addition to these theoretical tools, our reconfiguration testbed will demonstrate and validate these control algorithms and provide data to corroborate offline computations of the reconfiguration graph and power usage. The techniques and data from this research may enable new classes of reconfigurable space systems or enhance the capabilities of existing and next-generation space systems.

#### V. References

<sup>1</sup> Dong, S. et al. “Self-assembling wireless autonomously reconfigurable module design concept,” *Acta Astronautica*, Vol. 62, 2008, pp.246-256.

<sup>2</sup> McCamish, S.B., Romano, M., Nolet, S., Edwards, C.M., and Miller, D.W. “Ground and Space Testing of Multiple Spacecraft Control During Close-Proximity Operations.” AIAA Guidance, Navigation, and Control Conference, paper 2008-6664. AIAA, Washington, DC, 2008.

<sup>3</sup> Rui, C., Kolmanovsky, I., and McClamroch, N. H. “Nonlinear Attitude and Shape Control of Spacecraft with Articulated Appendages and Reaction Wheels.” *IEEE Transactions on Automatic Control*, Vol. 45, No. 8, 2000, pp.1455-1469.

<sup>4</sup> Rehnmark, F., Pryor, M., Holmes, B., Pedreiro, N., and Carrington, C.. “Development of a Deployable Nonmetallic Boom for Reconfigurable Systems of Small Modular Spacecraft,” 48<sup>th</sup> AIAA/SME/ASCE/AHS/ASC Structures, Structural Dynamics, and Materials Conference, AIAA, Washington, DC, 2007.

<sup>5</sup> Xia, C., Wang, P., and Hadaegh, F., “Optimal Formation Reconfiguration of Multiple Spacecraft with Docking and Undocking Capability,” *Journal of Guidance, Control, and Dynamics*, Vol. 30, No. 3, 2007, pp. 694-702.

<sup>6</sup> LeMaster, E., Schaechter, D., and Carrington, C., “Experimental Demonstration of Technologies for Autonomous On-Orbit Robotic Assembly,” Space 2006 Conference, AIAA, Washington, DC, 2006.

<sup>7</sup> Schaub, H., Parker, G. G. and King, L. B. “Challenges and Prospects of Coulomb Spacecraft Formations,” *Journal of the Astronautical Sciences*, Vol. 52, Nos. 1-2, 2004, pp. 169-193.

- <sup>8</sup> Kong, E.M.C, Kwon, D.W., Schweighart, S.A., Elias, L.M., Sedwick, R.J. and Miller, D.W. "Electromagnetic Formation Flight for Multi-Satellite Arrays." *Journal of Spacecraft and Rockets*, Vol 41, No. 4, 2004, pp. 659-666.
- <sup>9</sup> Shoer, J., and Peck, M. "Flux-Pinned Interfaces for the Assembly, Manipulation, and Reconfiguration of Modular Space Systems." AIAA Guidance, Navigation, and Control Conference, paper 2008-7233, AIAA, Washington, DC, 2008.
- <sup>10</sup> Shoer, J. and Peck, M. "Stiffness of a Flux-Pinned Virtual Structure for Modular Spacecraft," *Journal of the British Interplanetary Society*, 2009. (to appear)
- <sup>11</sup> Shoer, J. and Peck, M. "Reconfigurable Spacecraft as Kinematic Mechanisms Based on Flux-Pinning Interactions," *Journal of Spacecraft and Rockets*, 2009. (to appear)
- <sup>12</sup> Norman, M. "Stationkeeping of a flux-pinned satellite network." AIAA Guidance, Navigation and Control Conference and Exhibit, paper 2008-6475. AIAA, Washington, DC, 2008.
- <sup>13</sup> Jones, L. "Prospects and Challenges of Particulate Solar Sail Propulsion." AIAA/AAS Astrodynamics Specialist Conference and Exhibit, paper 2008-7077. AIAA/AAS, Washington, DC, 2008.
- <sup>14</sup> Gersh, J. "Architecting the Very-Large-Aperture Flux-Pinned Space Telescope: A Scalable, Modular Optical Array with High Agility and Passively Stable Orbital Dynamics." AIAA/AAS Astrodynamics Specialist Conference and Exhibit, paper 2008-7212. AIAA/AAS, Washington, DC, 2008.
- <sup>15</sup> Meissner, W. and Ochsenfeld, R. "Ein neuer Effekt bei Eintritt der Supraleitfähigkeit." *Die Naturwissenschaften*, Vol. 21, No. 44, 1933. pp.787-788.
- <sup>16</sup> Brandt, E. H., "Rigid levitation and suspension of high-temperature superconductors by magnets," *American Journal of Physics*, Vol. 58, No. 1, 1990, pp. 43-49.
- <sup>17</sup> Davis, L. C., "Lateral restoring force on a magnet levitated above a superconductor," *Journal of Applied Physics*, Vol. 67, No. 5, 1990, pp. 2631-2636.
- <sup>18</sup> Schonhuber, P. and Moon, P. C., "Levitation forces, stiffness, and force-creep in YBCO high- $T_c$  superconducting thin films," *Applied Superconductivity*, Vol. 2, No. 7, 1994, pp. 523-534.
- <sup>19</sup> Toumela, J. "Kinematic Analysis of Multibody Systems," *BIT Numerical Mathematics*, Vol. 48, No. 2, 2008, pp. 405-412.
- <sup>20</sup> Gu, E.Y.L. "Configuration Manifolds and Their Applications to Robot Dynamic Modeling and Control," *IEEE Transactions of Robotics and Automation*, Vol. 16, No. 5, 2000, pp.517-527.
- <sup>21</sup> Wittenburg, J. *Dynamics of Multibody Systems*. Springer, Berlin, 2007. pp. 116-117.
- <sup>22</sup> Baierlein, R. *Newtonian Dynamics*. McGraw-Hill, New York. 1983. pp. 161-162.
- <sup>23</sup> Liberzon, D. *Switching in Systems and Control*. Birkhauser, Boston. p. 56.
- <sup>24</sup> Henzinger, T.A. "The Theory of Hybrid Automata," *Proceedings of the 11th Annual Symposium on Logic in Computer Science (LICS)*, IEEE Computer Society Press, 1996, pp. 278-292.
- <sup>25</sup> Kordyuk, A. "Magnetic levitation for hard superconductors," *Journal of Applied Physics*, Vol. 83, No. 1, 1998, pp. 610-612.
- <sup>26</sup> Wilson, W., Shoer, J., and Peck, M. "Demonstration of a Magnetic Locking Flux-Pinned Revolute Joint for Use on CubeSat-Standard Spacecraft." AIAA Guidance, Navigation and Control Conference and Exhibit. AIAA, Washington, DC, 2009.